Eliminating Uncertainty of Driver's Social Preferences for Lane Change Decision-Making in Realistic Simulation Environment

Zejian Deng, Wen Hu, Chen Sun, Duanfeng Chu, Tao Huang, Wenbo Li, Chao Yu, Mohammad Pirani, Dongpu Cao, Amir Khajepour

***Abstract*—The task of making lane change decisions for autonomous vehicles in mixed traffic is intricate and challenging due to the uncertainty of surrounding vehicles. The uncertainty exists in terms of the diverse social driving preferences and unpredictable driving behavior of human drivers. To address these challenges, the decision-making process for changing lanes is represented as an incomplete information game, where the driver characteristics of surrounding vehicles are unknown during the interaction. To eliminate the uncertainty of the driving environment, the concept of driver aggressiveness is proposed to quantify the social driving preferences based on the Risk-Response (R-R) diagram in an explainable manner. Then the predicted trajectory is utilized to calculate the driving risks using Gaussian Mixture Model (GMM) that is trained by the naturalistic driving data in the interactive lane change scenarios extracted from the highD dataset. To make the simulation environment more diverse and realistic, the data-driven motion model social Intelligent Driver Model (SIDM) is constructed based on car-following data obtained from cut-in scenarios in the highD dataset. The simulations are conducted by setting up the environment vehicles equipped with SIDM model with diverse social driving preferences. The findings indicate that the proposed decision-making model can recognize the category of surrounding vehicles, and in realistic interactive driving scenarios, it can produce adaptive and human-like driving decisions.**

***Index Terms*—autonomous vehicle, lane change, game theory, driving preferences.**

I. Introduction

A. Background

AUTONOMOUS driving system is a breakthrough with a great potential to improve transportation and mobility [1]–[3]. Despite the prospects of autonomous vehicles, it is not feasible to replace human-driven vehicles soon. As a result, autonomous and human-driven vehicles will coexist in the predictable future. Consequently, autonomous vehicles must be included as a component of a multifaceted socio-technical system and be capable of socially compliant interaction with other traffic participants in the near future [4]–[6].

Lane change is a complex scenario in the highway driving that involves interacting with other human drivers in an unpredictable driving environment [7]. The objective functions of each vehicle in the interactions are interdependent. Moreover, the overall objective not only includes the balances of the driving safety and driving efficiency, but also includes the social norms, such as courtesy and cooperativeness, because driving is essentially a social task involving the appropriate interactions with each other [5], [8], [9].

B. Related Works

1) Rule-Based Methods

Rule-based approaches possess clear logic and low computational cost in making lane change decisions, and are widely used in the literature [10], [11]. MOBIL (Minimizing Overall Braking Induced by Lane Changes) model [12], for example, is a lane change model that makes decisions by considering the effects of lane change behavior. Gipps [11] initially introduced a conceptual framework that governs the decision-making process for lane changes. This framework considers the primary factors of possibility, necessity, and desirability when determining the timing, manner, and execution of a lane change.

2) Probabilistic Methods

To model the time-series decision-making with actions, states, rewards and transition probabilities, Markov decision process (MDP) is adopted [13]. Guan et al. [14] utilized MDP to model the driving task considering factors such as safety, efficiency, and comfort. As reinforcement learning (RL) can explore the driving environment with better scalability and generalization

This work was supported in part by the National Natural Science Foundation of China (52172393), the Natural Science Foundation of Hubei Province for Distinguished Young Scholars (2022CFA091), Wuhan Science and Technology Major Project (2022013702025184), Natural Sciences and Engineering Research Council (NSERC) of Canada, and in part by the technical and financial support of LoopX. (*Corresponding authors: Chen Sun, Duanfeng Chu.*)

Zejian Deng and Amir Khajepour are with the Department of Mechanical and Mechatronics Engineering, University of Waterloo, Waterloo, ON N2L3G1, Canada (e-mail: z49deng@uwaterloo.ca; a.khajepour@uwaterloo.ca).

Wen Hu and Dongpu Cao are with the School of Vehicle and Mobility, Tsinghua University, Beijing, China (e-mail: huwen@tsinghua.edu.cn; DP_Cao2016@163.com).

Chen Sun is with the Department of Data and Systems Engineering, University of Hong Kong, Hong Kong, China (e-mail: c87sun@hku.hk).

Duanfeng Chu is with the Intelligent Transportation Systems Research Center, Wuhan University of Technology, Wuhan 430063, China (e-mail: chudf@whut.edu.cn).

Tao Huang is with the School of Vehicle and Energy, Yanshan University, Yanshan, China (email: huangtao@chd.edu.cn)

Wenbo Li is with the College of Mechanical and Vehicle Engineering, Chongqing University, Chongqing 400044, China (e-mail: liwenbocqu@foxmail.com).

Chao Yu is with the LoopX, Waterloo, ON N2L6R5, Canada (email: chao.yu@loopx.ai).

Mohammad Pirani is with the Department of Mechanical Engineering, University of Ottawa, Ottawa, ON K1N6N5, Canada (e-mail: mpirani@uottawa.ca).

for problems modeled by MDP, it is widely studied in the field of autonomous driving decision-making [13], [15]–[17].

3) Game-Theoretic Methods

Recently, game theory is developed to deal with the interactions between human drivers by explicitly considering their dependencies. The objective functions of the involved players are coupled deeply, which shows the interaction dependency with each other. The game theoretical framework has been applied in the fields of economics [18], [19], biology [20], [21], computers science [22], [23], with solid mathematical foundations.

Game theory has been used in the highway driving research. Kita [24], [25] modelled merging behavior as a static complete information game, where the lane change was mandatory. Liao et al. [26] expanded upon Kita's research by examining merging behavior on highways using a two-player nonzero-sum game. Their work makes a significant contribution by considering the vehicles' anticipated states and actions in the payoffs that correspond to the decision-making procedure of human drivers. In contrast, the merging behavior is modeled by Kang et al. [27] as a single-instance game that initiates upon the entry of the ego vehicle into the merging lane. However, it lacks adaptability to the ever-changing characteristics of the surrounding traffic.

The uncertainty of the lane change interactions in the mixed traffic mainly stems from the unpredictable driving behaviors of the human drivers. Thus, the human attributes are introduced in the decision-making model, such as driving style [28]–[31] and Social Value Orientation (SVO) [5]. Driving style refers to a relatively stable characteristic manner, in which the driver chooses to drive or driving habits that have developed over time. SVO is a psychological concept that describes an individual's preference regarding the allocation of resources between themselves and others. In the context of driving, SVO reflects how much a driver prioritizes cooperative versus competitive behavior. Hang et al. [32]–[34] modelled both autonomous vehicle and human-driven vehicle as the rational agents that maximized their reward functions, where the weightings were assigned to driving safety, efficiency and comfort. The weightings were associated with different values by assuming human drivers' various preferences for the driving goals. However, the driving styles were defined without the support of driving behavior analysis of naturalistic driving data, which is unfounded. Moreover, the online driving style identification was not available for the autonomous vehicle, resulting in the inability of the decision-making model to adapt to other interactive vehicles. Compared to Hang's works, Schwarting et al. [5] enabled the autonomous vehicle drives in a more socially compatible manner, through introducing the SVO estimation module. However, the computational cost is high since they determined the SVO value using particle filter, especially when the number of surrounding vehicles increases.

4) Motion Model of Surrounding Vehicles

Another important challenge for related works is the lack of human-like intelligent agents as the interactive surrounding vehicles for the simulation, while claiming their models are interaction-aware. Specifically, the human drivers behave differently depending on the driving scenarios. Most lane change decision-making models require the lag vehicle to be realistic and imitate the human drivers' longitudinal driving behavior when they encounter the cut-in vehicle. Unfortunately, current studies use the rule-based motion models without considering the uncertainty and diversity of the surrounding vehicles, such as Intelligent Driver Model (IDM) and MOBIL models, or utility-based models in [32]–[34], while however, the weightings are determined subjectively. Then the decision-making models are difficult be adaptive to the real-vehicle testing.

C. Motivations and Contributions

From the literature review we can know that lane change decision-making for autonomous vehicles in mixed traffic is intricate and challenging due to the uncertainty of surrounding vehicles. Diverse social driving preferences and unpredictable driving behavior of human drivers create significant challenges for the decision-making tasks. Existing models often fail to capture the full spectrum of human driving behaviors, leading to suboptimal decision-making in dynamic environments. Moreover, the simulation environment is unrealistic and does not reflect real-world scenarios accurately, because the surrounding human-driven vehicles are controlled by the rule-based motion models without accounting for the diversity and interactions with human drivers.

To address the problems discussed above, this paper contributes to the current research as follows:

Firstly, the lane change decision is modelled as an incomplete information game, where the interactions and uncertainty of the human behavior are explicitly considered. Two-player and multiplayer games are applied to typical interactive lane change scenarios and large simulated interactive scenarios.

Secondly, considering the behaviors of the surrounding vehicles are not addressed in the published works, resulting in unrealistic interactions, this paper models the behaviors of the environment vehicles based on the real driving data, i.e., highD dataset [35]. The data-driven social IDM (SIDM) is proposed to make the simulation environment more realistic and interactive.

Thirdly, to eliminate the uncertainty of driving environment, the driver identification model is explored to determine the social driving preferences of the environment vehicles, which are distributed in the Risk-Response (R-R) diagram in an explainable manner. The modelled incomplete information game can then be solved by integrating the identification results of driver aggressiveness.

D. Paper Organizations

The paper is structured as follows. In Section II, the lane change decision-making problem is formulized. Section III introduces the motion model of environment vehicles. Section IV presents the driver identification model. The results are analyzed in Section V. Finally, this paper is concluded in Section VI.

II. Problem Formulization

A. General Lane Change Game Modelling

Game theory studies the strategic interactions among rational agents by employing mathematical models. A normal or strategic game is a triplet $\mathcal{G} = \langle \mathcal{I}, \mathcal{S}, \mathcal{P} \rangle$, where $\mathcal{I}$ is a non-empty set of players, consisted of individual player $i \in \mathcal{I}$. For player i, his strategies set is denoted by $S_i = \{s_i^1, \dots, s_i^{m_i}\}$, where m_i is

the total number of strategies. $P: \mathcal{S} \to \mathcal{I} \to \mathbb{R}$ is a function from strategy profiles to real-valued utilities. The player i's utility $u_i(s_i', s_{-i})$ is defined as the function of his strategy and the strategies of other players, where s_{-i} denotes the strategies of the other players, i.e., $s_{-i} = \{s_1, \dots, s_{i-1}, s_{i+1}, \dots, s_N\}$. Player i plays the game and chooses the best action by comparing the utilities in all possible results when the other players choose available actions. This best response of player i for a given action profile s_{-i} is defined as the action s_i^* such that $u_i(s_i^*, s_{-i}) \geq u_i(s_i, s_{-i})$ for all actions s_i. If the best response is achieved for all players, then the Nash equilibrium $s^* = (s_1^*, s_2^*, \dots, s_n^*)$ exists, that is, no player can increase its utility by unilaterally altering its strategy s_i^* such that

$$\boldsymbol{s}_i^* = \arg \max_{s_i \in S_i(s_{-i}^*)} u_i(\boldsymbol{s}_i, \boldsymbol{s}_{-i}^*), i = 1, \dots, n. \quad (1)$$

A general lane change scenario in highway is presented in Fig. 1, where several cars are regarded as the players. The autonomous vehicle is assigned as the ego vehicle (EV) marked by the red color, and the other surrounding vehicles are marked by the lighter colors, including leading vehicle (LEV), lag vehicle (LAV), front vehicle (FV) and following vehicle (FOV). Each vehicle has candidate actions $\{Lane\ Change, Lane\ Keeping\}$ in the lateral direction and $\{Yield, Acceleration\}$ in the longitudinal direction. The utility function of each player can denote the driving goal that the player tries to achieve, such as reducing the driving risks and improving driving speed. The detailed descriptions are presented in the Section II.B. The objective of the lane change game is to find the EV's driving decision based on the Nash equilibrium that each vehicle maximizes its driving goals. However, the uncertainty of the players exists in the real traffic, and could influence greatly the driving decision of the EV, which has not been considered yet. Thus, in the Section II.C, the uncertainty of each player will be discussed and the Bayesian equilibrium will be introduced.

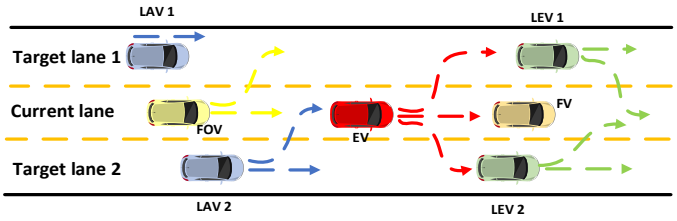

Fig. 1. Lane change interaction in the three-lane highway

B. Utilities Modelling of Players

From the observations in the real traffic, we can know that the drivers are required to follow the traffic rules, which are essentially designed to guarantee the driving safety. Simultaneously, the drivers normally pursue for higher speed to get to the destination earlier. Besides, the driving courtesy is necessary to be supplemented in the social driving tasks. Reducing the frequency of lane changes and stabilizing local traffic flow is a crucial aspect of demonstrating courtesy on the road [36], [37]. Frequent lane change increases the collision risks and discomforts the following vehicle in the adjacent lane. Therefore, the utility function is denoted as the driving goal that includes driving safety, higher driving efficiency and traffic flow stability, which are introduced as follows:

1) Driving Safety

Driving safety is essential as it directly impacts the likelihood of collisions and other hazardous situations. By prioritizing safety, the autonomous vehicle can make decisions that prevent accidents and protect itself and other road users. For vehicle i, its driving safety over a certain prediction horizon $\mathcal{T}$ is defined by the comparison between the inter-vehicle distance $d_{i,j}(t)$ and predefined threshold safety distance d_i^s, as well as the lane localization of each vehicle z_i and z_j. If the relative lane difference $z_{i,j}(t) = 0$ and $|d_{i,j}(t)| \geq d_i^s$ for all $t \in \mathcal{T}$, vehicle i is safe. The lane of a vehicle can be multiple if it is crossing the lane boundary. In this case, the vehicle i's safety can only be guaranteed when all the related vehicles satisfy the definition of driving safety.

In the definition above, $z_{i,j}$ is the relative lane difference $z_j - z_i$; $d_{i,j}(t)$ is the inter-vehicle distance at time t between vehicles i and j

$$d_{i,j}(t+1) = d_{i,j}(t) + \tau\big(v_j(t) - v_i(t)\big) \quad (2)$$

where $\tau > 0$ denotes the time interval; $v_i(t)$ and $v_j(t)$ are the longitudinal driving speeds of vehicles i and j at time t.

Many surrogate safety indicators have been used to quantify the safety level, such as time headway (THW), time to collision (TTC) and inter-vehicle distance. Besides, the response time of drivers to decelerate plays a critical role when the dangerous conditions happen. Therefore, these factors are integrated to the required deceleration, which is

$$a_{req,brake} = \frac{1}{2}(v_r + \rho a_r)^2 / [(d_{r,f} + \frac{v_f^2}{2a_{max,brake}}) - ((v_r\rho + \frac{1}{2}a_r\rho^2))] \quad (3)$$

Eq. (3) represents the required deceleration, $a_{req,brake}$, for the rear vehicle to avoid a collision under certain conditions. This indicator is the function of inter-vehicle distance $d_{r,f}$, the velocities of the front and rear vehicles v_f and v_r, the driver's reaction time ρ, the rear vehicle's acceleration a_r, and the maximum braking deceleration $a_{max,brake}$. In this formula, the term $(v_r + \rho a_r)^2$ represents the combined effect of the rear vehicle's current velocity and its acceleration over the driver's reaction time. The denominator consists of two parts: the effective stopping distance considering the front vehicle's velocity $(d_{r,f} + \frac{v_f^2}{2a_{max,brake}})$ and the distance covered by the rear vehicle during the reaction time $(v_r\rho + \frac{1}{2}a_r\rho^2)$. By incorporating these variables, Eq. (3) provides a comprehensive measure of the required deceleration needed to prevent a collision, taking into account the dynamic interaction between the vehicles and the driver's response characteristics.

The safety metrics, such as THW, TTC, relative distance, and relative speed, do not comprehensively represent driving safety. For instance, TTC is prone to sudden changes, and THW represents vastly different driving risks at different vehicle speeds. In contrast, our safety metric integrates multiple factors. Ultimately, these factors are combined into an interpretable physical variable—the required deceleration of the rear vehicle

to avoid collisions. This metric is not affected by the vehicle's speed and does not experience sudden changes. More importantly, it is an interpretable variable that can be used to explain driving safety based on the driving conditions.

Considering there are $N-1$ related vehicles around vehicle i, and the environment may change during the prediction horizon, the driving safety indicator is then determined as

$$\max\left(a_{req,brake,j}(t:t+\mathcal{T})\right), j = 1,2,\dots,N \tag{4}$$

The safety utility of vehicle i is then with the weight factor w_s

$$u_{i,safety} = w_s \max\left(a_{req,brake,j}(t:t+\mathcal{T})\right) \tag{5}$$

2) Driving Efficiency

Efficiency is another critical factor for the practical deployment of autonomous vehicles. An efficient driving strategy not only benefits the individual vehicle but also contributes to overall traffic flow. The driving efficiency of vehicle i is determined by the differences between current speed $v_i(t)$ and future speed $v_i(t+\mathcal{T})$, where the latter is vehicle speed in the long-term stable car-following state. Therefore, this term can be replaced by the speed of its future front vehicle j after the period $\mathcal{T}$. Meanwhile, the inter-vehicle distance $d_{i,j}(t+\mathcal{T})$ is also a factor that affects the $v_i(t+\mathcal{T})$. The vehicle i is free to accelerate to the limit speed v_{lim} if $d_{i,j}(t+\mathcal{T})$ is larger than the safe car-following distance d_i^s. Then the driving efficiency of vehicle i is formulated with the weighting w_e

$$u_{i,eff} = \begin{cases} w_e(v_j(t+\mathcal{T}) - v_i(t)) & d_{i,j}(t+\mathcal{T}) \le d_i^s \\ w_e(v_{lim} - v_i(t)) & d_{i,j}(t+\mathcal{T}) > d_i^s \end{cases} \tag{6}$$

3) Traffic-Friendly Factor

Traffic-friendly factor demonstrates the ability to interact harmoniously with human drivers and follow traffic norms, which is crucial for the acceptance and integration of autonomous vehicles into existing traffic systems. This factor ensures that the autonomous vehicle behaves in a socially acceptable manner, fostering trust and cooperation with other road users. In some conditions, the vehicle i may change lane even when the front vehicle is far, due to longer inter-vehicle distance from the leading vehicle in the other lane. However, this behavior may cause traffic flow oscillations and increase the collisions risks [36], [37]. Thus, the lane change frequency is limited to show traffic friendliness. A lane change will only be initiated if the current lane fails to fulfill the driving utilities. If the future required deceleration is less than the threshold a_{safe} in the current lane, a lane change penalty will be effective. Then the traffic-friendly factor is considered by the following term

$$u_{i,tff} = w_t\left(a_{safe} - \tilde{a}_{req,brake,i}\right) * \left(sgn\left(a_{safe} - \tilde{a}_{req,brake,i}\right) + 1\right) \tag{7}$$

where w_t is the weighting for traffic-friendly factor; a_{safe} is the threshold deceleration that ensures the driving safety; $\tilde{a}_{req,brake,i}$ is the predicted required deceleration calculated by Eq. (3) according to the future states of vehicle i, $sgn(\cdot)$ denotes the *sign function*.

C. Uncertainty of the Players

1) Bayesian Equilibrium Considering Player Type

The utilities of each player were analyzed and modelled for the lane change game in the previous sections. However, the uncertainty of the drivers was not considered yet, which greatly influence EV's driving decisions. Since the Vehicle-to-Vehicle (V2V) communication is not available in most current vehicles, the proposed game is incomplete information, and the player type matters. Two unfavorable conditions often happen between AVs and human-driven cars in the lane change interactions, i.e., overly cautious and overly aggressive decisions of the EV, due to the unavailability of driver type identification. The former case is especially often to see because the state-of-the-art AVs make driving decisions based on worst-case reasoning that ensures the driving safety against any controls the human might conduct.

A game of incomplete information is therefore proposed by $G = (\mathcal{I}, (S_i)_{i\in\mathcal{I}}, (\Theta_i)_{i\in\mathcal{I}}, (u_i(s,\theta))_{i\in\mathcal{I}}, p(\theta))$. Θ_i is a finite set of possible types of player i and $\Theta = X_{i\in\mathcal{I}}\Theta_i$ is the set of type assignments for all players, with a typical element $\theta = (\theta_i)_{i\in\mathcal{I}}$. Player i's type θ_i is chosen by nature (the pseudo player) through the probability mass function (*pmf*) p when the game starts. The player i estimates other players' types given its own type with the conditional probability distribution $p(\theta_{-i}|\theta_i)$. The utilities $u_i(s_i', s_{-i})$ defined in Section II.B then becomes the function of player type as $u_i(s_i', s_{-i}(\theta_{-i}), \theta_i, \theta_{-i})$.

The profile $(s_i(\cdot))_{i\in\mathcal{I}}$ is defined as a Bayesian game equilibrium if for player $i \in \mathcal{I}$ and player type $\theta_i \in \Theta_i$

$$s_i(\theta_i) \in \arg\max_{s_i'\in S_i} \sum_{\theta_{-i}} p(\theta_{-i} \mid \theta_i) u_i(s_i', s_{-i}(\theta_{-i}), \theta_i, \theta_{-i}) \tag{8}$$

2) Diverse Motion Models of Surrounding Vehicles

Considering the studied lane change scenarios are strongly interactive, the driving simulation is utilized for the model evaluation to avoid real driving risks in the on-field experiment. Therefore, the surrounding vehicles in the simulation environment are required to drive in a human-like manner, which is critical to the decision-making model evaluation. This process is considered by proposing a novel motion model supported by both car-following rules and naturalistic driving data, introduced in Section III. After the construction of realistic traffic environment, the autonomous vehicle will predict the trajectories of the surrounding vehicles, determine their social driving preferences, and integrate this information to make adaptive driving decisions, which are introduced in Section IV.

III. Data-Driven Motion Modeling of Environment Vehicles Based on HighD Dataset

To make the interactions in the simulation more diverse and realistic, the environment vehicles should behave like intelligent agents. In this research, the predominant motion state of surrounding vehicles is car-following. Consequently, this section proposes SIDM for car-following behavior modeling that integrates the classic IDM with naturalistic driving data. This integration allows us to model car-following behavior in a manner that more closely resembles that of human drivers.

A. Cut-in Scenarios Extraction from HighD Dataset

The highD dataset [35] comprises 16.5 hours of highway naturalistic driving data in the Cologne region of Germany, covering the years 2017 and 2018 and involving 110,000 vehicles. The dataset includes 60 recordings captured at six different locations along a 420-meter section of road, with a total duration of 16.5 hours.

To make the environment vehicles drive in a human-like manner, the car-following data of the LAV in cut-in interaction scenarios are analyzed. As depicted in Fig. 2, after the point T_1 when the EV starts to cut in, the LAV is compelled to drive behind the EV. The LAV observes the EV's dynamic behaviors, recognizes its turn signals, the distance between vehicles, the lateral position, etc. Based on these observations, the LAV implements appropriate longitudinal acceleration/deceleration control strategies to follow the EV while maintaining a safe distance.

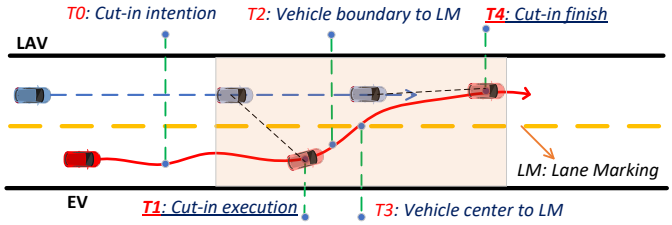

Fig. 2. Cut-in process division

Data from the time period $[T_1, T_4]$ allows us to discern human driver behavior when faced with a vehicle changing lanes in the right lane, as shown in the shaded area of Fig. 2. Based on this data, the car-following model can learn from the demonstrations of human drivers and interact with the lane-changing vehicle in a human-like manner. Consequently, the evaluation of the proposed model in a simulated environment will possess features of real-world traffic scenarios, including the diversity and uncertainty of interacting objects. This will make the validation results more convincing compared to previous works.

B. Driving Preferences Classification Based on an Explainable Way

The drivers are found to exhibit diverse car-following behaviors during cut-in interactions from the extracted data. Some drivers prefer to accelerate to vie for right-of-way with the lane-changing driver. Conversely, some drivers are more cautious, opting to decelerate and yield, which, despite sacrificing efficiency, greatly enhances driving safety. This diversity needs to be considered when modeling the motion of surrounding vehicles. To quantify the social preferences of car-following vehicles, we select relative distance, relative velocity, and longitudinal acceleration as driving indicators, and categorize drivers into aggressive, moderate, and cautious types. Unlike previous work, we do not use machine learning-based methods, such as clustering, for driver classification due to their lack of interpretability. Instead, we opt for an explainable approach. The advantage of this approach is that the classification is fully interpretable, and the driving preferences of drivers can be integrated into the car-following model in a very clear and understandable way, reflecting the diversity and uncertainty of surrounding vehicle behavior.

Based on the analysis above, we express the rules of driving preferences in the following mathematical formula.

$$a_{ij} \le f_{ij} \le b_{ij} \tag{9}$$

where, a_{ij} and b_{ij} are the upper and lower percentile of the driving features; f_{ij} is the jth feature of the ith driving preference; $i = 1,2,3$ represents the three different driving preferences, including cautious, moderate and aggressive drivers; $j = 1,2,3$ is the driving features, including relative distance, relative speed and acceleration.

In Eq. (9), we define the thresholds of various driving indicators for drivers with different driving preferences. Each type of driver should satisfy the defined thresholds simultaneously, which highlights the differences in their car-following behaviors.

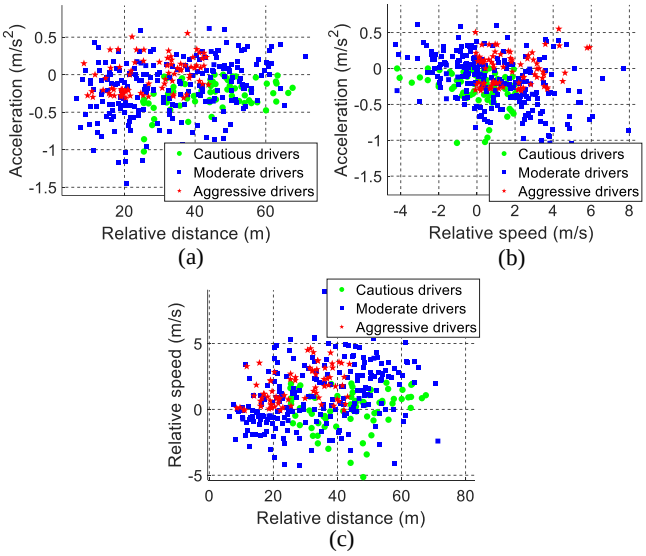

Fig. 3. Classification results of the driving preferences

Fig. 3 shows the classification results of driving preferences, categorized into cautious, moderate, and aggressive types. Overall, aggressive drivers, marked with red pentagrams, exhibit greater longitudinal acceleration, higher relative speed, and smaller relative distance to the front vehicle compared to moderate and cautious drivers. This categorization is further quantified by the mean values and variances of key driving features presented in the Table I. Aggressive drivers maintain an average relative distance of 27.87 m and a relative speed of 1.78 m/s. In contrast, cautious drivers keep a larger average relative distance of 44.95 m and have a lower relative speed of -0.04 m/s. These two types of drivers each account for about 20%. Moderate drivers, accounting for about 60% of the sample, exhibit intermediate behavior with an average relative distance of 37.10 m and a relative speed of 1.12 m/s.

Clearly, aggressive drivers pose higher driving risks during driving, which validates the reasonableness of the classification. Specifically, there is a clear range of driving feature distribution between aggressive and cautious drivers, even with some overlap. This is mainly to consider the proportion of each driving preference in the total sample, setting thresholds for driving preference boundaries. This classification of driving preferences provides support for the construction of the car-

following model in terms of diversity and uncertainty, enabling better simulation environment.

TABLE I

MEAN VALUES AND VARIANCES OF DRIVING FEATURES BY DRIVING PREFERENCES

Driving features	Mean values and variances		
	Cautious	Moderate	Aggressive
Relative distance	(44.95, 216.13)	(37.10, 849.91)	(27.87, 100.34)
Relative speed	(-0.04, 2.40)	(1.12, 6.17)	(1.78, 2.16)
Acceleration	(-0.31, 0.096)	(-0.24, 0.32)	(-0.01, 0.05)

C. Social IDM (SIDM) Construction Based on Real Data

The IDM model [38] is a renowned rule-based car-following model that has been applied in both traffic flow simulation software and autonomous driving simulation. However, the IDM model cannot reflect the heterogeneity of the driver population. Therefore, we introduce the analysis results of natural driving data to develop personalized car-following models for drivers with different car-following preferences, to emulate the actual car-following behaviors of human drivers. The IDM model is shown in Eq. (10).

$$a_{\mathrm{IDM}}(s, v, \Delta v) = a\left[1 - \left(\frac{v}{v_0}\right)^{\delta} - \left(\frac{s^*(v, \Delta v)}{s}\right)^2\right] \quad (10a)$$

where

$$s^*(v, \Delta v) = s_0 + vT + \frac{v\Delta v}{2\sqrt{ab}} \quad (10b)$$

The distance s between the ego vehicle and the front vehicle, the speed v of the front vehicle, and the speed difference Δv between the rear vehicle and the front vehicle are dynamic inputs, while the remaining variables are parameters that need to be predefined. s_0 is the minimum distance, v_0 is the desired speed, and T is the desired time headway, which are all positive. The comfortable deceleration b is designed to restrict the braking decelerations to a comfortable level.

To incorporate social factors, the parameter calibration of the SIDM relies on the classification results in Fig. 3. The features used for driving preference classification are also included in the IDM model, including input variables and output acceleration. Therefore, the SIDM will show significant differences based on this classification result. Similarly, the parameter set of the SIDM is also divided into three groups, with its parameter calibration based on the following equation.

$$\boldsymbol{\theta}_k = \underset{\boldsymbol{\theta}_k}{\operatorname{argmin}} \frac{1}{N} \sum_{i=1}^{N} (y_i - \tilde{y}_i(\boldsymbol{\Omega}|\boldsymbol{\theta}_k))^2 \quad (11)$$

The principle of SIDM parameter calibration is based on the metric of mean square error (MSE). By employing optimization techniques, we aim to minimize the average MSE between the time series data and the model's output. In doing so, we can obtain optimal parameters, ensuring that the model output closely fits the actual driving data. In the Eq. (11), At the ith time step denoted by i, the trajectory has a total number of observations represented by N. The parameters vector in the SIDM model is given by $\boldsymbol{\theta}_k = (v_0, T, s_0, a, b)^T$, while the measurement vector at the ith time step is represented by $\boldsymbol{\Omega} = (s(i), v(i), \Delta v(i))^T$. There are five parameters that need to be calibrated, which is difficult. However, it was mentioned in previous literature that the platoon oscillation stability [39] and variance contributions in the analysis of variance (ANOVA) [40] of car-following behavior are influenced by two important parameters: the desired time headway T and maximum acceleration a. Additionally, both studies have revealed that the most significant factor in enhancing car-following behavior is the adjustment of the desired time headway T. Therefore, we only calibrate the desired time headway T in this study.

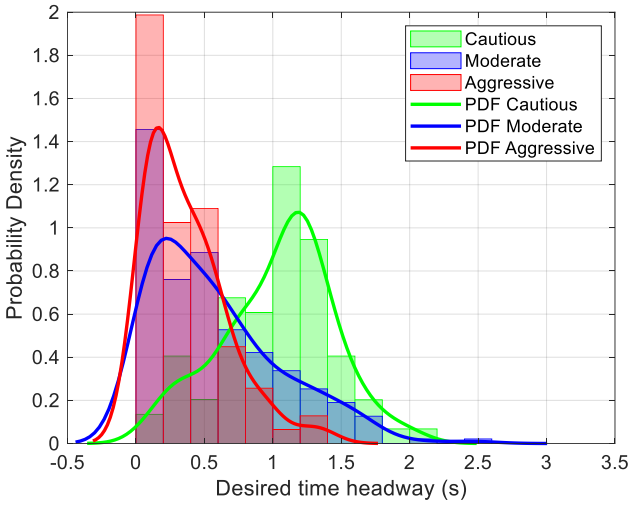

Fig. 4. Histograms and PDF curves of the desired time headway for different driving preferences

Fig. 4 presents the calibration outcomes, indicating that the calibrated desired time headway T among the three driver groups conforms to a normal distribution. The mean values of these distributions are 1.17 s, 0.7 s, and 0.41 s, respectively. It is worth noting that the findings indicate that more than 75% of cautious drivers have a desired time headway that exceeds that of 75% of moderate drivers and nearly all aggressive drivers. These findings are crucial for establishing different social driving preferences in the motion model of surrounding vehicles, thereby facilitating the evaluation of the decision-making model in real traffic conditions.

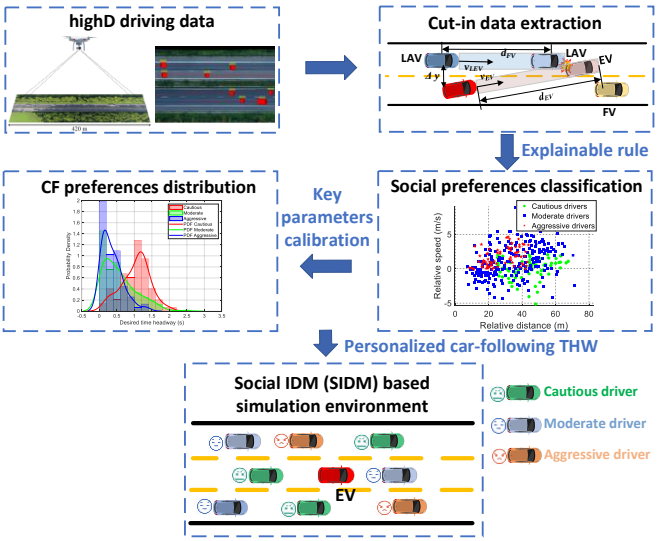

Fig. 5. Overall flow of the SIDM construction

Fig. 5 shows the overall flow of how the SIDM is constructed and applied in the autonomous driving simulation. First, the cut-in data were extracted from highD dataset. Then the social preferences of human drivers were classified based on the key driving features, including relative distance, relative speed and acceleration. The desired THW in the SIDM model was thereafter calibrated to show the car-following preferences when the cut-in happened. The SIDM-based simulation environment was finally constructed by placing surrounding vehicles with diverse driving preferences. The validation of the lane change decision-making model can be significantly enhanced as a result of the diversity and unpredictability of the surrounding vehicles within a realistic simulation environment.

IV. Identification of Social Driving Preferences

In this section, the driving preferences of surrounding vehicles are quantified in terms of driver aggressiveness. Then a driver identification model is proposed to eliminate the uncertainty of the driving environment for making safe and efficient driving decisions.

A. Driver Aggressiveness Quantifications

Two factors are considered to identify the driving preferences of a car-following driver, i.e., driving risks and driver's response, which is quantified by the longitudinal acceleration in the car-following scenario. An aggressive driver is expected to have higher acceleration when the driving risks are high (e.g., THW is low). Conversely, cautious drivers do not accelerate that much even in situations where the driving risks are low. The Risk-Response (R-R) diagram is therefore proposed to show the differences between aggressive and cautious drivers in Fig. 6. It is inspired by the stimulus-response model [41], which is a conceptual framework in psychology that describes how individuals respond to external stimuli. It was used to model the vehicle's car-following behavior, assuming the drivers react to stimuli from the environment. In our study, the stimulus is the driving risk that is quantified by the time headway between subject vehicle and leading vehicle. The response can also be obtained by measuring the vehicle acceleration. Thus, the ratio of response and stimulus, i.e., the slope in the R-R diagram, is taken as the parameter to quantify the driver aggressiveness. Overall, the R-R diagram is proposed by reversely using the widely adopted stimuli-response model. This quantification method for driver aggressiveness is appropriate and interpretable.

The longitudinal behavior of the LAV is not solely quantified by acceleration. This is because longitudinal behavior corresponding to the same acceleration can significantly vary if the vehicle's longitudinal speeds differ. To comprehensively take account into these influence factors, the future trajectories of the LAV are utilized to quantify the driver's longitudinal behavior.

Our initial hypothesis is that driver aggressiveness correlates with shorter time headway (THW) and larger accelerations. This hypothesis is grounded in previous research, which has demonstrated a significant relationship between these parameters and driver aggressiveness. Specifically, studies have shown that larger THW is indicative of more cautious driving behavior [42]–[44]. Conversely, greater accelerations under similar driving conditions are associated with more aggressive driving styles [45]–[47].

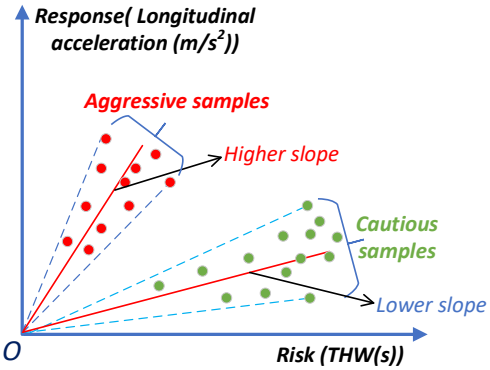

Fig. 6. Driver aggressiveness quantification based on R-R diagram

These findings are supported by extensive analyses of diverse driving datasets in these studies. This hypothesis is further validated using statistical analysis of the dataset. The THW and acceleration data are plotted for different driving styles in Fig. 7. The data shows that cautious drivers tend to have larger THW and smaller accelerations on average, whereas aggressive drivers exhibit shorter THW and larger accelerations. This statistical evidence supports the validity of using the R-R diagram model to define and identify driver aggressiveness.

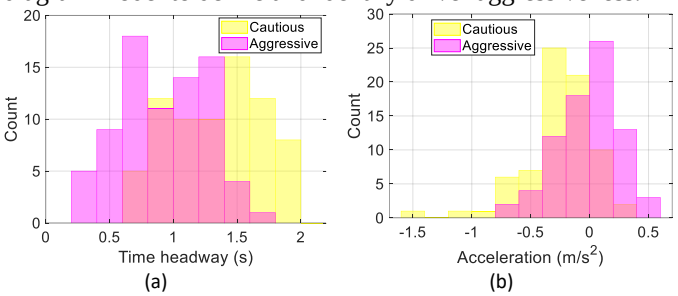

Fig. 7. Demonstrations of driving features between cautious and aggressive drivers. (a) Time headway, (b) Acceleration.

B. Interactive Trajectory Prediction of Surrounding Vehicles

The trajectory prediction of the target predicted car is conducted by extracting the information of its most relevant surrounding cars based on the Gaussian Mixture Model (GMM), considering its excellent approximation properties. The driving features selected for the GMM model include relative distance, relative speed, and acceleration, as these factors are critical in defining the motion patterns of surrounding vehicles. Firstly, relative distance between the ego vehicle and surrounding vehicles helps in understanding spatial relationships. Secondly, the speed is crucial for capturing dynamic interactions. The third parameter is the heading angle which allows the model to better capture the vehicle's orientation and directional intent.

The driving data utilized for training the GMM model are collected from naturalistic driving datasets during specific periods when interactions between the EV and the LAV are observed. Specifically, data are only used when the longitudinal time headway between the two vehicles is less than or equal to 2 seconds. This criterion ensures that the data captures meaningful interactions between vehicles, which is critical for the trajectory prediction model. The historical driving features of the LAV and EV are then used to predict the future motions of the LAV.

$$\boldsymbol{s}(\tau) = [v_{LAV}(\tau)\ \ \varphi_{LAV}(\tau)\ \ v_{EV}(\tau)\ \ \varphi_{EV}(\tau)\ \ \Delta d_x(\tau)\ \ \Delta d_y(\tau)], \tau \in [t - T_h, t] \quad (12)$$

where Δd_x and Δd_y represent distances between the LAV and EV in the longitudinal and lateral directions, separately. The historical horizon length is denoted by T_h. The model outputs are the anticipated velocity and yaw angle of the LAV:

$$\boldsymbol{z}(\mathrm{T}) = [v_{LAV}(\mathrm{T}) \quad \varphi_{LAV}(\mathrm{T})], \mathrm{T} \in [t, t + T_f] \quad (13)$$

The joint Gaussian mixture distribution is

$$p(\bar{x}) = \sum_{k=1}^{K} \pi_k N(\bar{\boldsymbol{x}} \mid \boldsymbol{\mu_k}, \boldsymbol{\Sigma_k}) \quad (14)$$

where $\bar{\boldsymbol{x}} = [\boldsymbol{s}(\tau), \boldsymbol{z}(\mathrm{T})]$; π_k, $\boldsymbol{\mu_k}$, $\boldsymbol{\Sigma_k}$ are the estimated weightings, mean value matrix and covariance matrix.

Then the driver response is determined based on the normalized occupancy of the predicted trajectory. The calculation for the percentage ratio is given by the following formula:

$$ratio = \frac{x_{GMM} - X_{min}}{X_{max} - X_{min}} \quad (15)$$

where x_{GMM} is the predicted trajectory generated by the trained GMM model $f_G(\cdot)$

$$x_{GMM}(t + T_f) = f_G(\boldsymbol{s}_{t-T_h:t}|\boldsymbol{\Phi}) \quad (16)$$

In Eq. (15), X_{min} and X_{max} are the minimum and maximum predicted distances the vehicle can travel, assuming it drives at the minimum and maximum accelerations, respectively. These values can be investigated using the available driving dataset. It is indicated from Fig. 8 that the LAV's predicted trajectory is normally distributed with an uncertainty range.

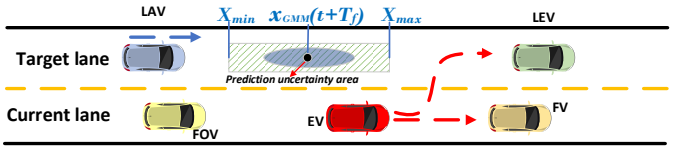

Fig. 8. Motion prediction with uncertainty

C. Lane Change Game Considering Driver Identification

Driver aggressiveness is defined by both the driving risk and the corresponding driver response. The former term is a determined value represented by the THW. The driver response is defined by the percentage ratio that follows the Gaussian distribution. Therefore, the i th driver aggressiveness χ_i is modeled as a random variable given by

$$\chi_i \sim \mathcal{N}(\mu_i, \delta_i^2) \quad (17)$$

The driver aggressiveness metric provides a clear indication of how a lane-changing vehicle adapts its behavior when interacting with other vehicles of varying aggressiveness. By utilizing Eq. (1), the utility of the EV can be evaluated in relation to the type of surrounding vehicles

$$w_1(\sigma_1, \dots, \sigma_N, \theta_1) := \int_{\mu_2-\delta_2}^{\mu_2+\delta_2} \dots \int_{\mu_N-\delta_N}^{\mu_N+\delta_N} f_{\mathrm{X}_2,\dots,\mathrm{X}_N}(\chi_2, \dots, \chi_N) v_1(\sigma_1, \dots, \sigma_N, \theta_1, \chi_2, \dots, \chi_N) d\chi_2 \dots d\chi_N \quad (18)$$

where $v_1(\sigma_1, \dots, \sigma_N, \theta_1, \chi_2, \dots, \chi_N)$ is the expected utility of the EV under the mixed strategy $\sigma_1 = (\sigma_{11}, \cdots, \sigma_{1K})$ and the other $N-1$ surrounding vehicles chooses the mixed strategy

$$(\sigma_2, \sigma_3, \dots, \sigma_N) = \begin{pmatrix} \sigma_{21} & \cdots & \sigma_{2J_2} \\ \vdots & \ddots & \vdots \\ \sigma_{N1} & \cdots & \sigma_{NJ_N} \end{pmatrix} \quad (19)$$

which is shown as

$$v_1(\sigma_1, \dots, \sigma_N, \theta_1, \chi_2, \dots, \chi_N) = \sum_{k=1}^{K} \sum_{j_2=1}^{J_2} \dots \sum_{j_N=1}^{J_N} \sigma_{1k}(\theta_1)\sigma_{2j_2}(\chi_2) \dots \sigma_{2j_N}(\chi_N) u_1(s_{1k}, s_{2j_2}, \dots, s_{Nj_N}) \quad (20)$$

where $\chi_2, \dots, \chi_N$ are the driver aggressiveness of the other $N-1$ surrounding vehicles, which are Gaussian random variables; The mixed strategies of players are denoted by $\sigma_1, \dots, \sigma_N$, while $f_{\mathrm{X}_2,\dots,\mathrm{X}_N}(\chi_2, \dots, \chi_N)$ signifies the joint probability density function (*pdf*) of the surrounding vehicles' driver aggressiveness. Given the utilities of each player under mixed strategies, the driving decisions can be determined by solving the game, and the optimal path is planned via polynomial splines [7].

V. Results and Discussion

A. Scenario 1: Two-Player Game

When the surrounding vehicles keep lane, the lane change becomes a two-player game, where the LAV and EV are the players. The LAV follows the SIDM while exhibiting distinct driving preferences, as discussed in Section III.

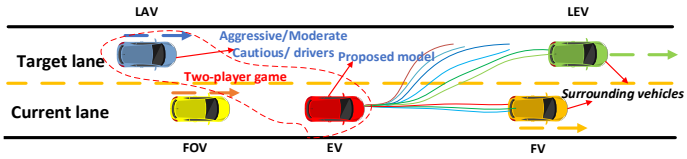

Fig. 9. The two-player lane change game with incomplete information

The lane width is set to 4 m. Each vehicle is 5 meters long and 2.2 meters wide. At the beginning of the simulation, the LAV operates under moderate driving preferences and maintains a normal following distance behind the EV. In each scenario, the vehicles' initial positions and longitudinal velocities are set to identical values. Light-colored bars are used to mark critical time steps in each figure. The benchmark utilized in this study is the game model that does not incorporate the driver identification module. The EV assumes that the LAV maintains moderate car-following preferences.

1) Interacting with a Cautious Driver

In this scenario, the FV and LEV are traveling at constant speed, and the LAV starts to drive cautiously when the EV intends to change lane at 9.7 s, as shown in Fig. 10 (a). As the

EV is driving faster than LAV, the cautious LAV decelerates accordingly, leading to a successful lane change with reduced risks. Once the lane change is complete, the new LAV and LEV are set up to be close to the EV in the leftmost lane, so the EV keeps lane until the simulation ends. As shown in Fig. 10 (b), the LAV's driver aggressiveness is observed to be around 0.4 for several seconds while it ranges from 0 to 1, because it drives moderately. After the LAV decelerates, its driver aggressiveness decreases to 0.25 in a short time period, showing the cautious driving preference. The EV thus performs a safe lane change until t=14.4 s.

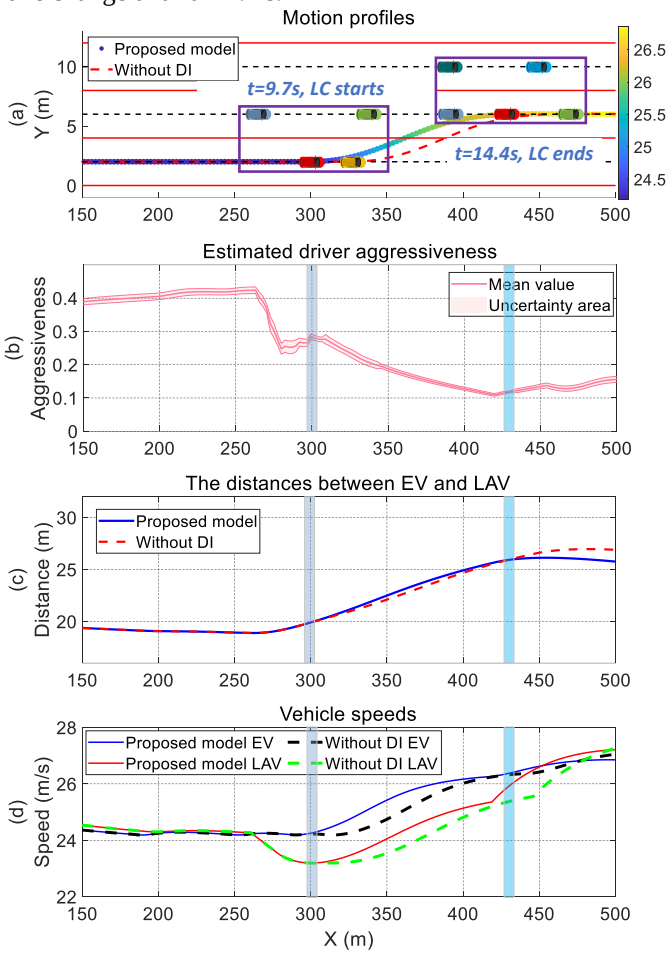

Fig. 10. Interactions with the cautious driver in the two-player game.

The identification of driver aggressiveness plays a crucial role in generating more efficient decisions. In the case of the benchmark without driver identification (DI), the EV initiates its lane change 1 s later than the proposed model, because the driver is not identified, which results in the conservative decision.

2) Interacting with an Aggressive Driver

The aggressive LAV's interactions are depicted in Fig. 11. At t=8.3 s, the LAV adopts an aggressive car-following preference. This prompts an acceleration in the LAV and a gradual reduction in the distance between the EV and the LAV. As driver aggressiveness escalates from approximately 0.5 to a higher level, the EV identifies the LAV's aggressive behavior. Consequently, the EV maintains its lane, following the FV at a stable speed without changing lanes. The proposed model demonstrates clear effectiveness in promoting safer driving decisions by determining the driving preferences.

The EV controlled by the game model without DI stays in its lane continuously because it assumes the LAV will drive moderately. This makes lane changing impossible even if the driver's perception is inaccurate.

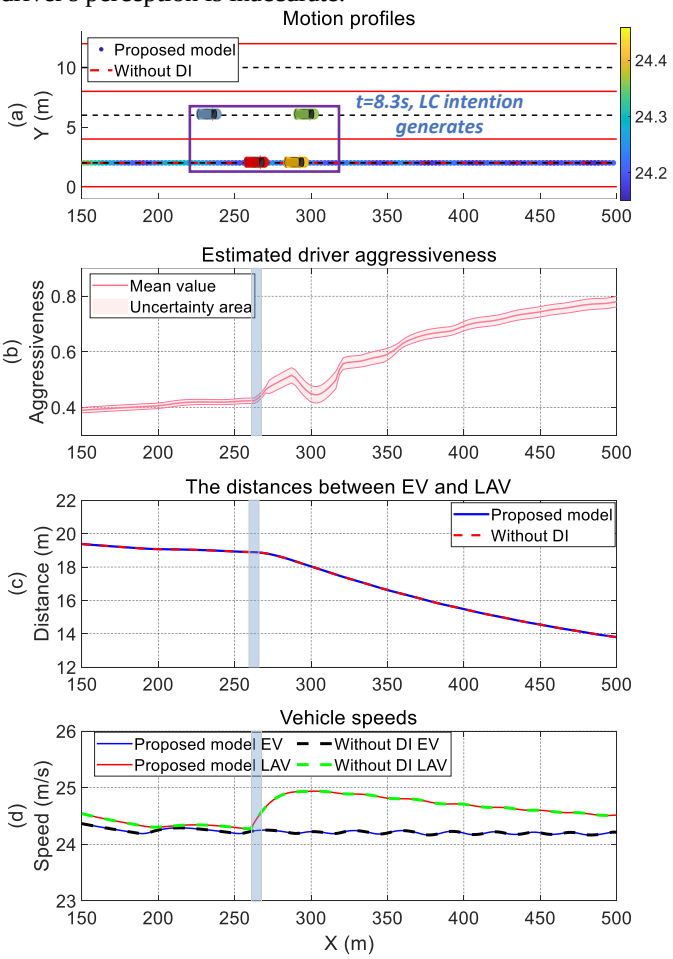

Fig. 11. Interactions with the aggressive driver in the two-player game.

B. Scenario 2: Multi-Player Game

In this scenario, the LEV cuts into the current lane, impacting other players' decisions, as shown in Fig. 12. The LAV is programmed to either yield to EV or accelerate. In the first case, the LAV follows the moderate SIDM model in the beginning and then yields to the EV. In the other case, the LAV is manually controlled to surpass the EV.

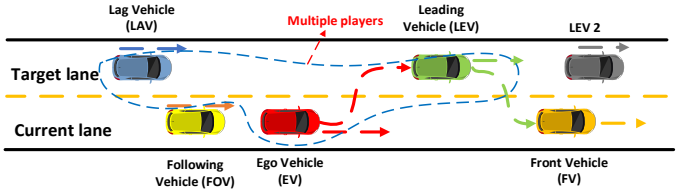

Fig. 12. The multi-player lane change game with incomplete information

1) LEV Cuts in and LAV Yields

The EV and LEV's motion profiles are depicted in Fig. 13. Notably, the LEV's cut-in process is marked by a square marker, while the EV's corresponding positions are denoted by a pentagram. At the beginning of the experiment, there are

multiple LAVs positioned behind the EV. The first LAV, being very close to the EV, accelerates and overtakes the EV, becoming the LEV when it cuts in front of the EV. The LEV prompts the EV to change lanes prematurely. The second LAV, which follows, is the vehicle that yields to the EV.

Our prior work [7] presents the quantifications of driving risks, taking into account THW, TTCi (inverse TTC), and relative distance. As Fig. 13 (b) shows, the risk levels and the inter-vehicle distances encounter a sudden change when the original LAV overtakes the EV replacing the old LEV, and cuts into the current lane to become the new FV. Thus, the desire for lane change increases. Concurrently, the new LAV's driving preference transitions from moderate to cautious, enlarging the inter-vehicle distance between EV and LAV. As a result, the EV successfully changes lanes from t=4.4 s to t=10.1 s.

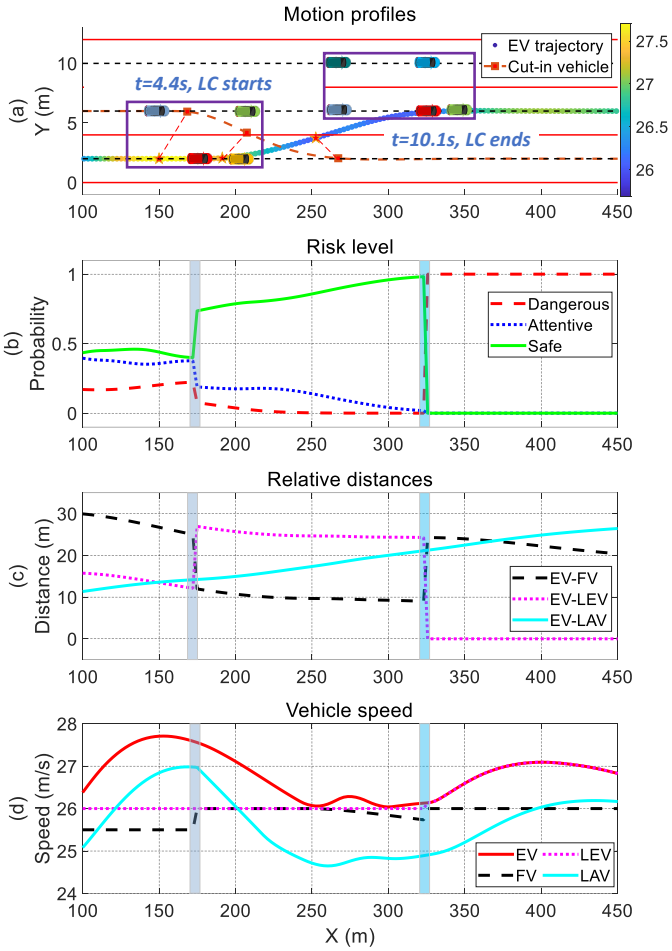

Fig. 13. Interactions with the cautious lag vehicle when the LEV cuts in.

2) LEV Cuts in and LAV Accelerates

As illustrated in Fig. 14, the motion of the other vehicles and driving conditions remain the same as the last case, while however, the new LAV in the target lane accelerates to overtake the EV. The distance between EV and LAV continues to shorten and the safety-danger probability difference slowly decreases, after the EV's lane change. The EV subsequently returns back at t=6.5 s considering the distance is 10 m from LAV. The LAV continues accelerating, surpassing the EV at t=10.5 s, and the simulation terminates. It is found that the driver identification module helps the EV evaluate the driving risks from the environment vehicles and avoid the collisions.

C. Validations Based on Human Driving Data

Human driving data are extracted from highD dataset for the validation of the proposed model through comparing the driving decisions and generated trajectories. Two scenarios are studied, where the LEV maintains its lane and cuts in, respectively.

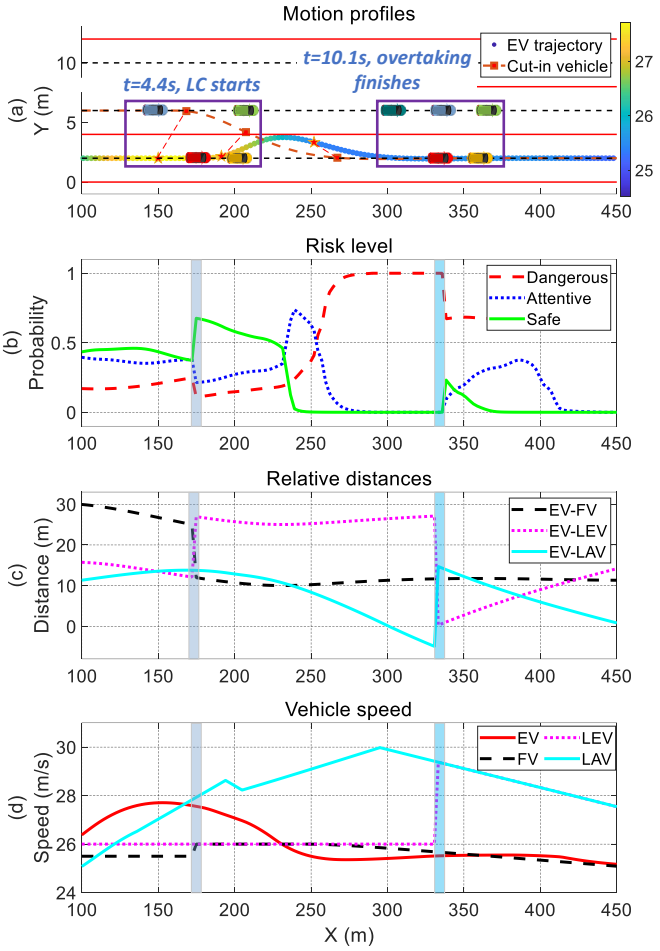

Fig. 14. Interactions with the aggressive lag vehicle when the LEV cuts in.

1) LEV Keeps Lane

In this scenario, the LEV does not cut in, and the game is played by only EV and LAV, as shown in Fig. 15. The EV initially accelerates due to the large EV-FV distance, while the human driver decelerates and yields to the LEV. As the EV gets closer to the FV, it keeps lane and slows down because the LAV drives very close, and the danger probability is 1. Since the human-controlled EV decelerates initially, the EV-LAV distance is then large enough for a lane change. Hence, the lane change maneuver happens earlier. In terms of the total traveling distance, the proposed model stops at 424.85 m, while the human-controlled car travels 413.03 m, indicating higher efficiency of the proposed model.

2) LEV Cuts in

In this scenario, the LEV cuts into the current lane, and the interactions happen among the LEV, EV and LAV, as shown in Fig. 16. The EV initially accelerates due to the large distance to

the FV. As the LEV starts cutting in, the EV slows down to yield to the LEV. Subsequently, the EV initiates a lane change maneuver without being affected by the LAV and LEV. For the human-driven EV, it conducts similar driving strategy to the proposed model. It is shown that the motion profiles of two controlled EVs are close. In terms of driving efficiency, the total traveling distances are 412.4 m and 412.7 m for the multi-player game model and human-driven vehicle. This indicates a comparable level of driving efficiency between the two.

The validations reveal that the proposed model prioritizes exploring the current lane before considering changing lane, as opposed to human drivers who can make longer-term predictions. Furthermore, human drivers behave variously, and a range of vehicle trajectories exist in the naturalistic driving dataset. In comparison to human drivers, the proposed model ensures driving safety while achieving similar driving efficiency.

D. Statistical Comparisons with Baselines

To better validate the proposed decision-making model, three baselines are selected, including the game theoretic model without driver identification (NO-DI), optimization-based Model Predictive Control (MPC), and Deep Reinforcement Learning model based on Deep Q-Network (DQN-DRL). Additionally, we generate 120 scenarios for each of the cautious, moderate, and aggressive social driving preferences based on the proposed SIDM model, resulting in a total of 360 scenarios. This controls the interaction behavior of the LAV with the EV in these random lane change scenarios. Collision rate (CR), lane change success rate (SR), and average speed (AS) are selected as evaluation metrics, and the results are shown in Table II.

The results show that our method outperforms the benchmark methods under different conditions. The driver identification module enables our method to avoid collisions in all scenarios. Moreover, the proposed method can generate adaptive driving behaviors by identifying the driving characteristics of the LAV. This provides a way to maintain a good balance between safety and efficiency. Without considering driver identification, the safety, lane change success rate, and driving efficiency of the model are reduced in all scenarios.

TABLE II

STATISTIC RESULTS OF THE PROPOSED METHOD COMPARED WITH BASELINES

LAV type	Methods	CR (%)	SR (%)	AS (m/s)
Cautious	Ours	0	95.83	27.24
	NO-DI	2.50	93.33	26.96
	MPC	5.83	88.33	26.46
	DQN-DRL	1.67	92.50	26.91
Moderate	Ours	0	89.50	26.56
	NO-DI	6.67	87.50	26.38
	MPC	13.33	78.33	25.24
	DQN-DRL	5.83	89.17	26.46
Aggressive	Ours	0	85.83	26.32
	NO-DI	10.83	83.33	26.04
	MPC	17.50	72.50	24.89
	DQN-DRL	9.17	86.67	26.41

The MPC benchmark method exhibits the driving behavior that lacks efficiency when interacting with a cautious LAV, because it is based on a constant speed prediction for the LAV. Additionally, the MPC benchmark performs poorly under all settings, with high collision rates, low lane change success rates, and low driving efficiency. The reasons may include a lack of interaction in the strategy, only specifying a fixed safety distance constraint. Compared to the MPC method, the DRL benchmark significantly reduces the collision rate. However, it ignores the uncertainty of the environment vehicles in decision-making, resulting in some collisions and lower driving efficiency compared to the proposed model.

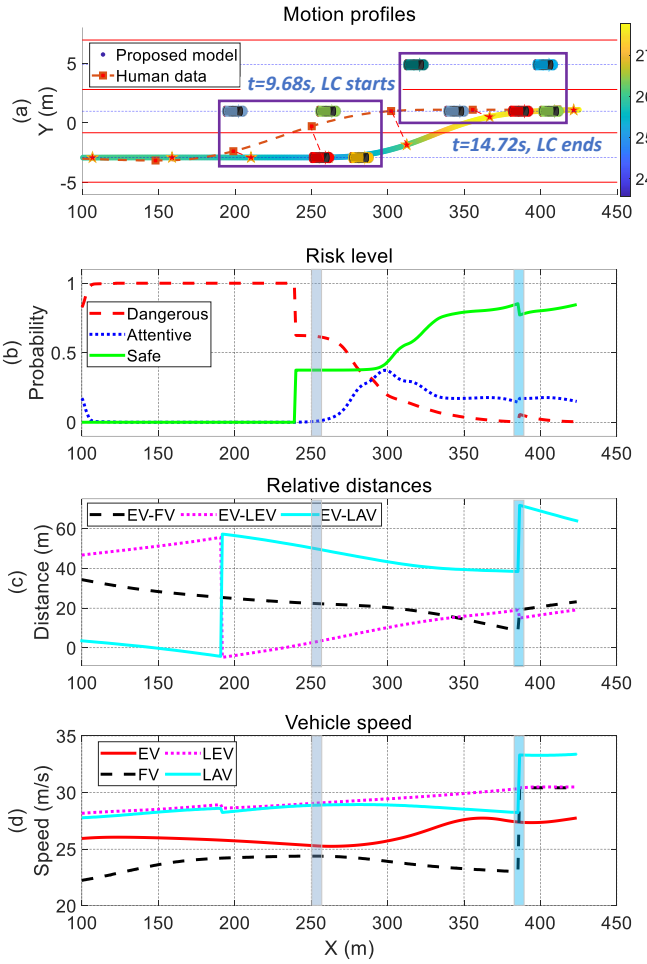

Fig. 15. The comparisons between the human driver and proposed model when LEV keeps lane.

E. Discussions

The performances of the proposed model are evaluated in the realistic simulation environment, where the surrounding vehicles are equipped with the data-driven SIDM model. Also, the validations are conducted by utilizing the driving environment in the highD dataset.

In the first case, the two-player game is modelled when the LEV keeps lane. The interactions are studied between the autonomous vehicle and both cautious and aggressive LAVs. Compared to the benchmark model, the proposed model identifies the driving preferences of other vehicles and makes driving decisions adaptively with higher safety and efficiency. In the second case, the multi-player game is formulated when the LEV cuts in to the EV's driving lane. Then the EV is forced to change lane due to the sudden drop of the driving space. The LAVs are switched to the decelerating and overtaking types in

two separate scenarios. Based on the proposed decision-making model, the EV can select different car to follow with higher expected driving efficiency and lower driving risks. It should be noted that the internet of things [48] and driver intent prediction [49] technologies are helpful for the proposed decision-making model, because the autonomous vehicle needs to get the necessary information of surrounding vehicles in the decision-making process.

Besides the simulations, the validations are also conducted. Two typical scenarios are selected from the highD dataset, where the LEV maintains lane and changes lane, respectively. Therefore, the two-player and multi-player games are both included in the validations. Similar safety and efficiency performances are found in the comparisons between the proposed model and human driving data, although there are differences in the trajectories. Overall, human-like decision-making frameworks for autonomous vehicles help achieve better interaction with human drivers in mixed traffic environments, and help the proposed model to exhibit more natural driving behaviors [42].

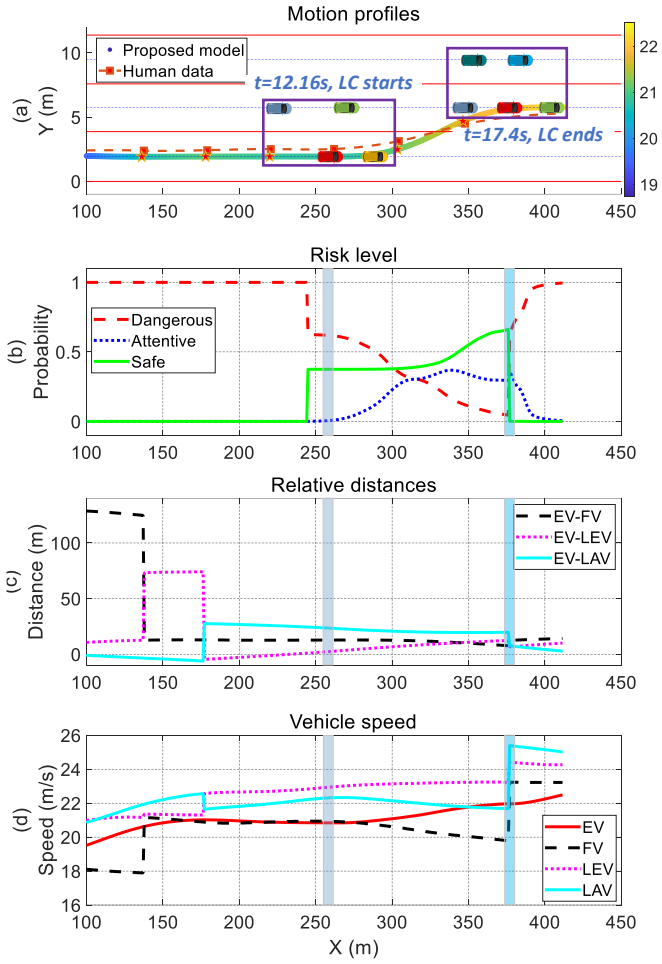

Fig. 16. The comparisons between the human driver and proposed model when LEV cuts in.

While the driver identification model helps the decision-making model make more adaptive driving decisions in simulation environments, several challenges should be addressed for successful real-world implementation. These include robust data acquisition and processing, model adaptation, and computational efficiency. These challenges are worth exploring in future research to help improve the effectiveness of the proposed model in real-world autonomous driving scenarios.

VI. Conclusions and Future Work

This paper modelled lane change decision-making based on game theory, considering interactions with the diverse human-driven vehicles in the mixed traffic. Two-player and multi-player games were applied to possible interactive lane change scenarios in real driving. The SIDM motion model was proposed to connect the motions of surrounding vehicles to human driving behavior by integrating the IDM model and real driving data. As a result, the interactions in the simulations were more realistic and comprehensive compared to existing studies. By introducing the R-R diagram, the social driving preferences were defined and quantified in an explainable manner. With the development of driver identification, the proposed model could recognize the aggressiveness of surrounding drivers. The simulations and validations demonstrated that the proposed decision-making model could make human-like driving decisions to enhance driving safety and efficiency.

In the future work, the players in the game can be irrational, and the decision results will be different. Additionally, it is worth investigating the incorporation of traffic rules and constraints into the research to ensure driving decisions comply with traffic regulations. Future research will also focus on collecting comprehensive datasets that include road and weather conditions and developing mechanistic models to integrate these factors effectively. Moreover, field tests in a controlled and safe environment will be conducted to further demonstrate the practical applicability of our model.

Appendix

A. *The calculation of the Bayesian Nash equilibrium*

An incomplete information game is constructed where each player adopts mixed strategies, determining each action according to a certain probability distribution. According to Nash's proof [50], any game with a finite number of players and a finite number of actions has a mixed-strategy Nash equilibrium. In this game, the number of players and actions are both finite, so an equilibrium solution must exist.

When solving this game, there may be multiple equilibria. An equilibrium selection mechanism is used by considering both payoff dominance and risk dominance strategies to select among multiple Nash equilibria [51], [52]. For example, if in Equilibrium 1, the payoff of each player is higher than that in all other equilibria, the AV's driving decision will be made based on Equilibrium 1. If the above condition is not met, the equilibrium is selected with the minimum driving risk for the AV and use its result as the driving decision. This condition is easy to achieve because the AV only needs to drive conservatively. As the experiment progresses, the AV will re-evaluate the driver aggressiveness of surrounding vehicles and make safe and efficient driving decisions.

After the lane change decision-making and driver aggressiveness identification, the utility functions are established for each vehicle. Thereafter, the Bayesian Nash

equilibrium is solved using the sequential quadratic programming (SQP)-based quasi-Newton technique [53]. This problem is transformed into the following optimization problem:

$$\begin{aligned} &\min \sum_{i\in N} [\beta^i - u^i(\sigma)] \\ &s.t.\ u^i\left(\sigma^{-i}, s_j^i\right) - \beta^i \leqslant 0 \quad \forall j = 1,\dots,m^i, \forall i \in N \\ &\sum_{j=1}^{m^i} \sigma_j^i = 1 \qquad\qquad \forall i \in N \\ &\sigma_j^i \geqslant 0 \qquad\qquad \forall j = 1,\dots,m^i, \forall i \in N \end{aligned} \tag{21}$$

where β^i is the optimal payoff of the player i. $u^i(\sigma)$ is the payoff to player i when all players play mixed strategies. The calculated strategy combination σ is the one that makes each player have a payoff value that is close to the highest possible value as much as possible. $\left(\sigma^{-i}, s_j^i\right)$ denotes the mixed strategies combination in which player i plays with his j_{th} pure strategy. m^i is the number of pure strategies that player i has. σ_j^i denotes the probability assigned to pure strategy s_j^i. After optimization, the calculated strategy combination σ is the one that makes each player have a payoff value that is close to the highest possible value as much as possible. It is proved that this strategy combination σ is just a Nash equilibrium of the game studied. Detailed proof has been provided in [53].

Take **x** to be a vector of length $m+n$ described as follows. Arranging the strategies of players 1 to n in order, we have a total of m strategies and we take x_i in order as: $x_1 = \sigma_1^1, x_2 = \sigma_2^1, \dots, x_{m^1} = \sigma_{m^1}^1, \dots, x_m = \sigma_{m^n}^n$, where subscripts in σ denote the strategies and superscripts stand for the players. Then take $x_{m+i} = \beta^i, i = 1,2,\dots,n$. Performing this transformation of variables in Eq. (21), it is converted to the following form

$$\begin{aligned} min \quad & f(\mathbf{x}) \\ s.t. \quad & g(\mathbf{x}) \leq 0 \\ & h(\mathbf{x}) = 0 \\ & x_i \geq 0\ \forall i = 1,\dots,m \\ & x_i\ are\ unrestricted \\ & \forall i = m+1, m+2 \dots, m+n \end{aligned} \tag{22}$$

where

$$\begin{aligned} f(\mathbf{x}) &= \sum_{i\in N} (\beta^i - u^i(\sigma)) \\ g(\mathbf{x}) &= u^i\left(\sigma^{-i}, s_j^i\right) - \beta^i \quad \forall j = 1,2,\dots,m^i, \forall i \in N \\ h(\mathbf{x}) &= \sum_{j=1}^{m^i} \sigma_j^i - 1 \quad \forall i \in N \end{aligned}$$

Eq. (22) is the standard form of a nonlinear optimization problem. To get a solution of this nonlinear minimization problem with nonlinear constraints, we use the SQP-based quasi-Newton method. The readers can refer to [54] for a detailed description of the method.

B. Experimental Parameters

The experimental parameters are listed in the following table.

TABLE III
DETAILS OF THE EXPERIMENTAL PARAMETERS

Parameter	Value (unit)	Description
w_s	5	Weighting for driving safety
w_e	3	Weighting for driving efficiency
w_t	1.5	Weighting for driving courtesy
v_{lim}	35 m/s	Maximum vehicle speed
ρ	1 s	Driver's reaction time
$a_{max,brake}$	2 m/s^2	Maximum braking deceleration of preceding vehicle
v_0	32 m/s	Desired speed in IDM
s_0	10 m	Minimum distance in IDM
L	100 m	Maximum detection distance
l_{veh}	5 m	Vehicle length
w_{veh}	2.2 m	Vehicle width
T_p	3 s	Trajectory prediction horizon

REFERENCES

[1] J. Wu, Q. Kong, K. Yang, Y. Liu, D. Cao, and Z. Li, "Research on the steering torque control for intelligent vehicles co-driving with the penalty factor of human-machine intervention," *IEEE Trans. Syst. Man, Cybern. Syst.*, 2022.

[2] B. Li *et al.*, "Sharing Traffic Priorities via Cyber–Physical–Social Intelligence: A Lane-Free Autonomous Intersection Management Method in Metaverse," *IEEE Trans. Syst. Man, Cybern. Syst.*, 2022.

[3] C. Hu *et al.*, "RISE-based integrated motion control of autonomous ground vehicles with asymptotic prescribed performance," *ieee Trans. Syst. man, Cybern. Syst.*, vol. 51, no. 9, pp. 5336–5348, 2019.

[4] J. Wei, J. M. Dolan, and B. Litkouhi, "Autonomous vehicle social behavior for highway entrance ramp management," in *2013 IEEE Intelligent Vehicles Symposium (IV)*, 2013, pp. 201–207.

[5] W. Schwarting, A. Pierson, J. Alonso-Mora, S. Karaman, and D. Rus, "Social behavior for autonomous vehicles," *Proc. Natl. Acad. Sci.*, vol. 116, no. 50, pp. 24972–24978, 2019.

[6] L. Müller, M. Risto, and C. Emmenegger, "The social behavior of autonomous vehicles," in *Proceedings of the 2016 ACM International Joint Conference on Pervasive and Ubiquitous Computing: Adjunct*, 2016, pp. 686–689.

[7] W. Hu *et al.*, "Probabilistic Lane-change Decision-Making and Planning for Autonomous Heavy Vehicles," *IEEE/CAA J. Autom. Sin.*, 2022.

[8] W. Wang, L. Wang, C. Zhang, C. Liu, and L. Sun, "Social interactions for autonomous driving: A review and perspectives," *Found. Trends® Robot.*, vol. 10, no. 3–4, pp. 198–376, 2022.

[9] D. Bissell, T. Birtchnell, A. Elliott, and E. L. Hsu, "Autonomous automobilities: The social impacts of driverless vehicles," *Curr. Sociol.*, vol. 68, no. 1, pp. 116–134, 2020.

[10] P. Hidas, "Modelling vehicle interactions in microscopic simulation of merging and weaving," *Transp. Res. Part C Emerg. Technol.*, vol. 13, no. 1, pp. 37–62, 2005.

[11] P. G. Gipps, "A model for the structure of lane-changing decisions," *Transp. Res. Part B Methodol.*, vol. 20, no. 5, pp. 403–414, 1986.

[12] A. Kesting, M. Treiber, and D. Helbing, "General lane-changing model MOBIL for car-following models," *Transp. Res. Rec.*, vol. 1999, no. 1, pp. 86–94, 2007.

[13] Y. He, L. Xing, Y. Chen, W. Pedrycz, L. Wang, and G. Wu, "A generic Markov decision process model and reinforcement learning method for scheduling agile earth observation satellites," *IEEE Trans. Syst. Man, Cybern. Syst.*, 2020.

[14] Y. Guan, S. E. Li, J. Duan, W. Wang, and B. Cheng, "Markov probabilistic decision making of self-driving cars in highway with random traffic flow: a simulation study," *J. Intell. Connect. Veh.*, 2018.

[15] S. Mo, X. Pei, and C. Wu, "Safe reinforcement learning for autonomous vehicle using monte carlo tree search," *IEEE Trans. Intell. Transp. Syst.*, 2021.

[16] K. Zheng, H. Yang, S. Liu, K. Zhang, and L. Lei, "A Behavior Decision Method Based on Reinforcement Learning for Autonomous Driving," *IEEE Internet Things J.*, vol. 9, no. 24, pp. 25386–25394, 2022.

[17] X. Xu, L. Zuo, X. Li, L. Qian, J. Ren, and Z. Sun, "A reinforcement learning approach to autonomous decision making of intelligent

vehicles on highways," *IEEE Trans. Syst. Man, Cybern. Syst.*, vol. 50, no. 10, pp. 3884–3897, 2018.
[18] R. J. Aumann and S. Hart, *Handbook of game theory with economic applications*, vol. 1. North-Holland Amsterdam, 1992.
[19] T.-M. Choi, A. A. Taleizadeh, and X. Yue, "Game theory applications in production research in the sharing and circular economy era," *International Journal of Production Research*, vol. 58, no. 1. Taylor & Francis, pp. 118–127, 2020.
[20] P. Hammerstein and R. Selten, "Game theory and evolutionary biology," *Handb. game theory with Econ. Appl.*, vol. 2, pp. 929–993, 1994.
[21] M. Archetti and K. J. Pienta, "Cooperation among cancer cells: applying game theory to cancer," *Nat. Rev. Cancer*, vol. 19, no. 2, pp. 110–117, 2019.
[22] T. Roughgarden, "Algorithmic game theory," *Commun. ACM*, vol. 53, no. 7, pp. 78–86, 2010.
[23] Y. Zhou, M. Kantarcioglu, and B. Xi, "A survey of game theoretic approach for adversarial machine learning," *Wiley Interdiscip. Rev. Data Min. Knowl. Discov.*, vol. 9, no. 3, p. e1259, 2019.
[24] H. Kita, "A merging–giveway interaction model of cars in a merging section: a game theoretic analysis," *Transp. Res. Part A Policy Pract.*, vol. 33, no. 3–4, pp. 305–312, 1999.
[25] H. Kita, K. Tanimoto, and K. Fukuyama, "A game theoretic analysis of merging-giveway interaction: a joint estimation model," *Transp. Traffic Theory 21st Century*, pp. 503–518, 2002.
[26] X. Liao *et al.*, "Game theory-based ramp merging for mixed traffic with unity-sumo co-simulation," *IEEE Trans. Syst. Man, Cybern. Syst.*, 2021.
[27] K. Kang and H. A. Rakha, "Game Theoretical Approach to Model Decision Making for Merging Maneuvers at Freeway On-Ramps," *Transp. Res. Rec. J. Transp. Res. Board*, vol. 2623, no. 1, pp. 19–28, 2017, doi: 10.3141/2623-03.
[28] M. Kuderer, S. Gulati, and W. Burgard, "Learning driving styles for autonomous vehicles from demonstration," in *Proceedings - IEEE International Conference on Robotics and Automation*, Jun. 2015, vol. 2015-June, no. June, pp. 2641–2646, doi: 10.1109/ICRA.2015.7139555.
[29] Z. Deng *et al.*, "A Probabilistic Model for Driving-Style-Recognition-Enabled Driver Steering Behaviors," *IEEE Trans. Syst. Man, Cybern. Syst.*, 2020.
[30] Z. Deng, D. Chu, C. Wu, Y. He, and J. Cui, "Curve safe speed model considering driving style based on driver behaviour questionnaire," *Transp. Res. part F traffic Psychol. Behav.*, vol. 65, pp. 536–547, 2019.
[31] D. Chu, Z. Deng, Y. He, C. Wu, C. Sun, and Z. Lu, "Curve speed model for driver assistance based on driving style classification," *IET Intell. Transp. Syst.*, vol. 11, no. 8, 2017, doi: 10.1049/iet-its.2016.0294.
[32] P. Hang, C. Huang, Z. Hu, Y. Xing, and C. Lv, "Decision making of connected automated vehicles at an unsignalized roundabout considering personalized driving behaviours," *IEEE Trans. Veh. Technol.*, vol. 70, no. 5, pp. 4051–4064, 2021.
[33] P. Hang, C. Lv, C. Huang, Y. Xing, and Z. Hu, "Cooperative decision making of connected automated vehicles at multi-lane merging zone: A coalitional game approach," *IEEE Trans. Intell. Transp. Syst.*, vol. 23, no. 4, pp. 3829–3841, 2021.
[34] P. Hang, C. Lv, Y. Xing, C. Huang, and Z. Hu, "Human-like decision making for autonomous driving: A noncooperative game theoretic approach," *IEEE Trans. Intell. Transp. Syst.*, vol. 22, no. 4, pp. 2076–2087, 2020.
[35] R. Krajewski, J. Bock, L. Kloeker, and L. Eckstein, "The highd dataset: A drone dataset of naturalistic vehicle trajectories on german highways for validation of highly automated driving systems," in *2018 21st International Conference on Intelligent Transportation Systems (ITSC)*, 2018, pp. 2118–2125.
[36] Z. Zheng, S. Ahn, D. Chen, and J. Laval, "The effects of lane-changing on the immediate follower: Anticipation, relaxation, and change in driver characteristics," *Transp. Res. part C Emerg. Technol.*, vol. 26, pp. 367–379, 2013.
[37] P. Chauhan, V. Kanagaraj, and G. Asaithambi, "Understanding the mechanism of lane changing process and dynamics using microscopic traffic data," *Phys. A Stat. Mech. its Appl.*, vol. 593, p. 126981, 2022.
[38] M. Treiber, A. Hennecke, and D. Helbing, "Congested traffic states in empirical observations and microscopic simulations," *Phys. Rev. E*, vol. 62, no. 2, p. 1805, 2000.
[39] J. Sun, Z. Zheng, and J. Sun, "The relationship between car following string instability and traffic oscillations in finite-sized platoons and its use in easing congestion via connected and automated vehicles with IDM based controller," *Transp. Res. Part B Methodol.*, vol. 142, pp. 58–83, 2020.
[40] B. Ciuffo, V. Punzo, and M. Montanino, "Global sensitivity analysis techniques to simplify the calibration of traffic simulation models. Methodology and application to the IDM car-following model," *IET Intell. Transp. Syst.*, vol. 8, no. 5, pp. 479–489, 2014.
[41] R. Rac-Lubashevsky, A. Cremer, A. G. E. Collins, M. J. Frank, and L. Schwabe, "Neural index of reinforcement learning predicts improved stimulus–response retention under high working memory load," *J. Neurosci.*, vol. 43, no. 17, pp. 3131–3143, 2023.
[42] T. Zhang, J. Zhan, J. Shi, J. Xin, and N. Zheng, "Human-like decision-making of autonomous vehicles in dynamic traffic scenarios," *IEEE/CAA J. Autom. Sin.*, vol. 10, no. 10, pp. 1905–1917, 2023.
[43] B. Gao, K. Cai, T. Qu, Y. Hu, and H. Chen, "Personalized adaptive cruise control based on online driving style recognition technology and model predictive control," *IEEE Trans. Veh. Technol.*, vol. 69, no. 11, pp. 12482–12496, 2020.
[44] P. Sun, X. Wang, and M. Zhu, "Modeling car-following behavior on freeways considering driving style," *J. Transp. Eng. Part A Syst.*, vol. 147, no. 12, p. 4021083, 2021.
[45] P. Jardin, I. Moisidis, S. S. Zetina, and S. Rinderknecht, "Rule-based driving style classification using acceleration data profiles," in *2020 IEEE 23rd International Conference on Intelligent Transportation Systems (ITSC)*, 2020, pp. 1–6.
[46] B. Zhu, Y. Jiang, J. Zhao, R. He, N. Bian, and W. Deng, "Typical-driving-style-oriented personalized adaptive cruise control design based on human driving data," *Transp. Res. part C Emerg. Technol.*, vol. 100, pp. 274–288, 2019.
[47] Y. Zhu *et al.*, "A framework for combining lateral and longitudinal acceleration to assess driving styles using unsupervised approach," *IEEE Trans. Intell. Transp. Syst.*, 2023.
[48] Q. Zhao, G. Li, J. Cai, M. Zhou, and L. Feng, "A tutorial on internet of behaviors: Concept, architecture, technology, applications, and challenges," *IEEE Commun. Surv. Tutorials*, vol. 25, no. 2, pp. 1227–1260, 2023.
[49] Y. Rahman, A. Sharma, M. Jankovic, M. Santillo, and M. Hafner, "Driver Intent Prediction and Collision Avoidance With Barrier Functions," *IEEE/CAA J. Autom. Sin.*, vol. 10, no. 2, pp. 365–375, 2023.
[50] J. F. Nash Jr, "Equilibrium points in n-person games," *Proc. Natl. Acad. Sci.*, vol. 36, no. 1, pp. 48–49, 1950.
[51] P. Février and L. Linnemer, "Equilibrium selection: payoff or risk dominance?: the case of the 'Weakest Link,'" *J. Econ. Behav. Organ.*, vol. 60, no. 2, pp. 164–181, 2006.
[52] M. Punniyamoorthy, S. Abraham, and J. J. Thoppan, "A Method to Select Best Among Multi-Nash Equilibria," *Stud. Microeconomics*, vol. 11, no. 1, pp. 101–127, 2023.
[53] B. Chatterjee, "An optimization formulation to compute Nash equilibrium in finite games," in *2009 Proceeding of International Conference on Methods and Models in Computer Science (ICM2CS)*, 2009, pp. 1–5.
[54] R. Fletcher, *Practical methods of optimization*. John Wiley & Sons, 2000.

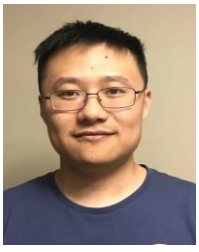

Zejian Deng received his Ph.D. degree in Mechanical and Mechatronics Engineering from the University of Waterloo in 2022, the M.A.Sc degree in Transportation Engineering and the B.Sc. degree in Automation from Wuhan University of Technology in 2018 and 2015. He is currently working as a postdoctoral fellow in Mechatronic Vehicle Systems Lab at the University of Waterloo. His research interests include driver

model, driving safety validations, decision-making, planning and control in automated driving.

Wen Hu earned the B.S. and M.S. degrees from Hunan University, Changsha, China, in 2015 and 2018, respectively. He is currently pursuing his Ph.D. degree in Mechanical Engineering at the College of Mechanical and Vehicle Engineering, Hunan University. His research interests include decision making and trajectory planning, vehicle dynamics and control in intelligent vehicle.

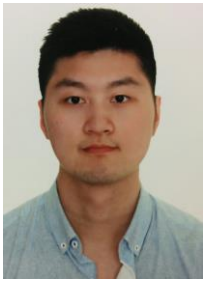

Chen Sun received the Ph.D. degree in Mechanical & Mechatronics Engineering from University of Waterloo, ON, Canada in 2022, M.A.Sc degree in Electrical & Computer Engineering from University of Toronto, ON, Canada in 2017 and B.Eng. degree in automation from the University of Electronic Science and Technology of China, Chengdu, China, in 2014. He is currently an Assistant Professor with the Department of Data and Systems Engineering, University of Hong Kong. His research interests include field robotics, safe and trustworthy autonomous driving and in general human-CPS autonomy.

Duanfeng Chu received the B.E. and Ph.D. degrees in mechanical engineering from Wuhan University of Technology, Wuhan, China, in 2005 and 2010, respectively. He is currently a professor with the Intelligent Transportation Systems Research Center, Wuhan University of Technology, focusing on the research of autonomous and connected vehicle and intelligent transportation systems.

Tao Huang received his Ph.D. degree in School of Automobile, Chang'an University in 2024. He spent one year as a visiting scholar at University of Waterloo from 2023 to 2024.

He is currently a lecturer at the School of Vehicle and Energy, Yanshan University. His research interests include autonomous driving, driver's intention, human-machine collaboration control, and vehicle active safety.

Wenbo Li received the B.S., M.Sc. and Ph.D. degree in automotive engineering from Chongqing University, Chongqing, China, in 2014, 2017 and 2021, respectively. From January 2022 to January 2024, he was a Postdoctoral Research Fellow with Tsinghua University. He is currently an Associate Professor with Chongqing University, Chongqing, China. His research interests include intelligent vehicle, intelligent cockpit, human emotion and cognition, human-machine interaction, affective computing, brain-computer interface.

Chao Yu is the co-founder and CEO of LoopX, a Canadian AI and robotics company revolutionizing safety and productivity in the mining industry. He holds a Ph.D. from the University of Waterloo, where his research focused on machine learning-based motion planning and control for autonomous vehicles.

Mohammad Pirani received his B.Sc. degree in Mechanical Engineering from Amirkabir University of Technology in 2011 and M.A.Sc. degree in Electrical and Computer Engineering and Ph.D. degree in Mechanical and Mechatronics Engineering from the University of Waterloo in 2014 and 2017, respectively. He is currently an Assistant Professor with the Department of Mechanical Engineering, University of Ottawa, Canada. His research interests include resilient and fault-tolerant control, networked control systems, and multi-agent systems.

Dongpu Cao received his Ph.D. degree from Concordia University, Canada, in 2008. He is a Professor at Tsinghua University. His current research focuses on driver cognition, automated driving and cognitive autonomous driving. He has contributed more than 200 papers and 3 books. He received the SAE Arch T. Colwell Merit Award in 2012, IEEE VTS 2020 Best Vehicular Electronics Paper Award and 6 Best Paper Awards from international conferences.

Amir Khajepour received his Ph.D. degree from the University of Waterloo, Waterloo in 1996. He is currently a professor of Mechanical and Mechatronics Engineering at the University of Waterloo. He holds Tier 1 Canada Research Chair in Mechatronic Vehicle Systems and Senior NSERC/General Motors Industrial Research Chair in Holistic Vehicle Control. His work has resulted in training over 150 PhD and MASc students, 30 patents, 600 publications, many technology transfers, and several start-up companies. He is a recipient of the Engineering Medal from the Professional Engineering Ontario, a fellow of the Engineering Institute of Canada, the American Society of Mechanical Engineering, and the Canadian Society of Mechanical Engineering.